AIRBORNE LASER PROFILING OF ANTARCTIC ICE STREAM FOR CHANGE DETECTION

Blue Spikes, Bea Csatho, Ian Whillans
Byrd Polar Research Center, The Ohio State University, 1090 Carmack Rd. Columbus, OH 43210
[spikes.2, csatho.1, whillans+]@osu.edu

KEY WORDS: Antarctica, Laser Altimetry, Accuracy, Repeatability, Ice Stream, and Mass Balance

ABSTRACT

The mass balance of ice in Antarctica is a prime need in science. The ice sheets are major variables in the global budget that controls sea level. It could be that thinning of the ice sheets accounts for the current rate of rise of sea level. There is a limited suite of techniques available for measuring mass-balance in Antarctica. A report is presented on the first of intended repeat surface mapping from an aircraft with GPS position determination and a downward-looking laser ranger. This method has the great merit of being precise and of covering large regions. Moreover, laser flights are used to make topographic maps and describe the shape of unusual portions of the ice sheet. The detection of special surface features raises the possibility of some mechanical understanding of ice sheet change.

1. INTRODUCTION

Laser altimetry is expected to solve many central problems in Antarctica. A major concern is how ice thickness may be changing and affecting global sea level. A deeper issue is locating the source of ice thickness change and determining its propagation style so that the cause and effect of changes may be deduced. Studies have shown laser altimetry to be a valuable tool in mapping and monitoring glacier thickness in Alaska (Echelmeyer et al., 1996; Adalgeirsdóttir et al., 1998) and Greenland (Csatho et al., 1996; Krabill et al, 1995; Garvin and Williams, 1993; Krabill et al., 1999). The use of laser altimetry to monitor changes occurring in Antarctica is the subject of the present contribution.

This report addresses first results of precision airborne laser altimetry in Antarctica. First flights were conducted during the 1997-98 austral summer. Repeat flights are scheduled for January 2000. Data from the first flights have been used to make surface maps of four fast-flowing regions of West Antarctica, although only the results from Ice Stream C are presented here. There are numerous flight-to-flight crosses with one another to assess repeatability. Other flights cross areas surveyed using snowmobile mounted GPS to assess system accuracy. Long baseline accuracy is determined using flights that go near mass-balance measurement sites known as coffee-cans that are part of another study (Hamilton et al., 1998 and Hamilton, pers. comm.). Future surveys of the same regions will be used to determine elevation changes over time.

2. WORK AREA

Unique features of West Antarctica, known as ice streams, are the focus of this study (Fig. 1). The ice streams are the major conduits that drain West Antarctica. They are located to the east of the Ross Sea meeting the Ross Ice Shelf along the Siple Coast. The ice streams are broad, typically around 50 km, and long, usually greater than 500 km, zones of rapid water-lubricated flow. Unlike mountain glaciers, the ice streams do not follow bedrock troughs. The ice streams are separated by ice ridges that may be frozen to underlying bedrock. The details of how ice streams operate are not well understood. However, some of these ice streams are known to be changing very quickly with time (Hamilton et al., 1998; Bindschadler and Vornberger, 1998; Joughin et al., 1999; Hamilton, pers. comm.). The cause for the changes is a topic of some debate within the science community.

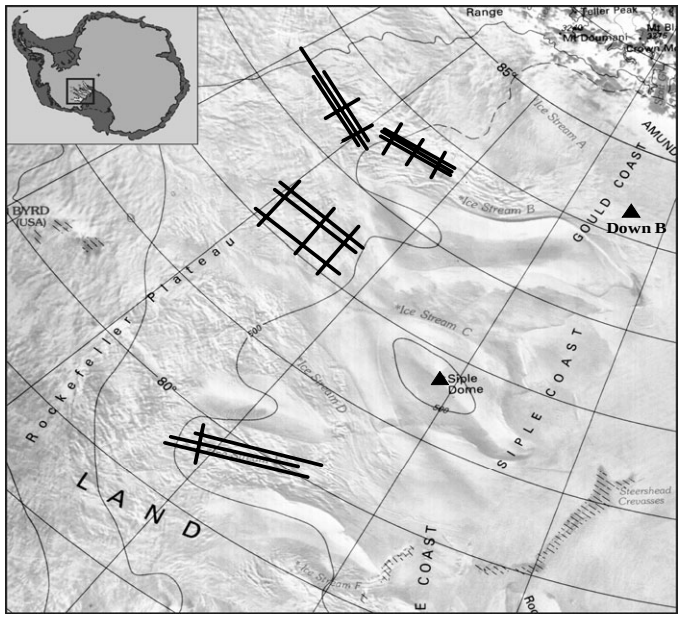

Fig. 1. Inset is a map of Antarctica with the location of the ice stream region enclosed in a black box. The large map is an enlargement of the ice stream region with laser survey lines (black grids) superimposed over a mosaic of advanced very high resolution radiometer imagery (Mullins, 1999).

3. DESCRIPTION OF LASER ALTIMETRY SYSTEM

Equipment is mounted on a ski-equipped Twin Otter aircraft that is operated by the NSF-SOAR (National Science Foundation-Support Office for Aerogeophysical Research) facility. The geophysical systems on board include a

gravimeter, magnetometer, a laser altimeter and an ice-penetrating radar. Positional information is provided by differential Global Positioning System (GPS), supplemented by Inertial Navigation System (INS), and precision pressure altimetry data. During most of the surveys performed by SOAR all sensors are collecting data allowing to map the ice sheet surface, the internal layering of the ice and the bedrock geometry and composition simultaneously. However, only the laser system, the ice-penetrating radar and auxiliary equipments were used during our laser altimetry missions. The altimetric measurements are made while the aircraft flies over a pre-determined flight path guided by real-time GPS.

3.1 Base Station Positioning

Two Ashtech dual frequency receivers located at different base camps are used as static base stations. The origin of each flight determines which base station is used. One of these base stations is located on a very slow moving (0.34 m/a) portion of the ice-sheet known as Siple Dome (Fig. 1). A survey of this nearly static base station was performed on the first and last day of flying. Positions with an overall RMS of 0.02 m were acquired using the Automated GIPSY system developed by Jet Propulsion Laboratory. Ice motions at this site are small and uncomplicated, so time-linear interpolation is used to determine the position of the base station for the intermediate days. Another base station is located at the Down-B camp located near the middle of Ice Stream B (Fig. 1). The ice there moves at a rate of over 500 m/a. The position of the Down-B receiver relative to the Siple Dome receiver is computed using GPSurvey processing software (Trimble Inc.). A position is determined for each flight originating at Down-B. The calculated horizontal position of this station changes in a linear fashion as expected (Fig. 2a). The calculated vertical position of the station changes in an irregular manner (Fig. 2b). This magnitude of elevation change is not characteristic of an ice sheet over such short distances and is most likely an error in the GPS positioning due to the long baseline between receivers (280 km) and the horizontal movement of the Down-B receiver during each survey. The elevation of this base station is estimated to be the mean from five out of six surveys with an RMS of 0.065 m. The calculated position of the sixth survey is considered an outlier because it deviates from the mean by more than four times the reported RMS and is therefore not used (Fig. 2).

3.2 Aircraft Positioning

Once the base station position is established, the relative position of the Ashtech or TurboRogue receiver on the aircraft is calculated using GPSurvey. Shi and Cannon (1995) showed that the accuracy of GPS positioning on a moving aircraft can be at the 0.10 m level if tropospheric, ionospheric, precise satellite orbits (ephemerides), and multipath corrections are used during differential carrier phase post-processing (Shi and Cannon, 1995). GPSurvey software is used for processing and found to be reliable when used on a computer with a large amount of memory and a fast processor. For 11 out of twelve flights the maximum RMS reported by GPSurvey is 0.10 m. The 12th flight was not used, because phase ambiguities were not resolved for a large portion of the flight.

To assess the performance of the GPSurvey processing, one survey was processed with GUITAR (GPS Inferred Trajectories for Aircrafts and Rockets, courtesy of John Sonntag, EG & G). The two solutions agree well, having a maximum difference of 1 cm in the horizontal and 8 cm in the vertical.

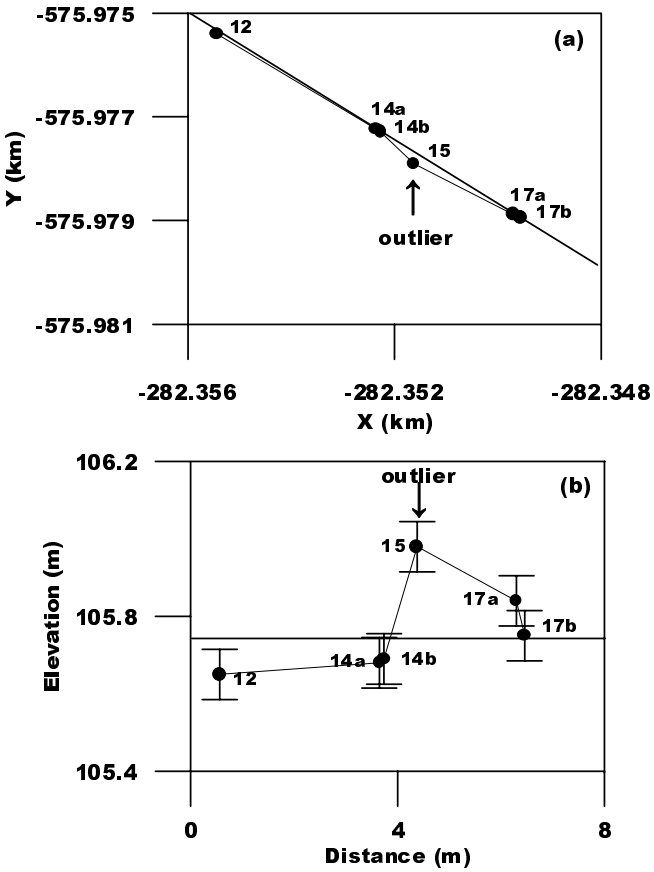

Fig. 2. (a) Measured changes in horizontal position of the Down-B receiver. The points are labeled according to the day of the year that the survey took place. Two surveys, a and b, were conducted on days 14 and 17. Black line is a linear best fit through the data calculated without the point marked "outlier". The X and Y coordinates are polar stereographic. (b) Elevation of each Down-B position plotted versus horizontal movement. Black line is the mean, elevation calculated without the point marked "outlier". Error bars are based on a 1-sigma RMS about the mean elevation.

3.3 Laser Ranging

The Azimuth LRY 500 is a diode pumped Nd:YAG pulsed laser transceiver, operating in the near infrared domain (1064 nm). Pulsed lasers measure the travel time of a laser pulse from the laser firing point to the surface and back to the receiver. To measure the time between the transmitted and the received pulses the Azimuth LRY 500 rangefinder uses 50% constant fraction discrimination. The timer starts at some consistent point on each transmitted pulse. Each timing event ends when the return pulse strength reaches half of its maximum amplitude. Thus the need of "range walk" correction is

eliminated. The manufacturer reports a single pulse accuracy of 0.1m for distances up to 1.7 km. The ranger records at 500 Hz and 64 pulses are averaged to yield one range. The beam divergence was set for 4.5 mrad, producing a footprint with 1.5 meter diameter from the 300 m nominal flight height. This results in one average elevation for every 1.5 by 8 m area when the aircraft flies at 300-m terrain clearance.

3.4 Aircraft attitude

The attitude of the aircraft, that is the heading, pitch, and roll angles determine the pointing direction of the laser. These angles are measured with a laser gyroscope that is part of the Litton Aero Products LTN-92 INS unit. The INS has a quoted accuracy of 0.05^{o} in all three angles (Vaughn et al., 1996), which translates to less than a 0.06 m error in calculated surface elevations when the aircraft is flying at less than 300 meters terrain clearance and the off-nadir pointing angles are less than 15^{o}. These angles are not exceeded during survey missions, so the measured attitude contributes very little to the overall error budget.

3.5 System timing

Each data collecting system operates independently and not in synchrony with the others. Universal Coordinated Time (UTC) is used as the standard to which all other times are corrected. The laser and INS measurements are tagged by a counter time that is corrected to UTC using information provided by the GPS time code generator. An additional correction is required for the individual attitude parameters, because the INS only records one angle at a time. The manufacturer specifies that these time lags are as follows: 110 ms in true heading, 60 ms in pitch and 50 ms in roll for the LTN-92 (Vaughn et al., 1996). It is possible to check whether these values are correct using pitch and roll maneuvers over a flat test field because timing offsets cause deformation of the measured surface when off-nadir angles are large. When performed, this test yielded slightly different time lags of 60 ms in roll and 85 ms in pitch. The measured time lags are preferred over the reported ones. The final step in correlating the data streams is to interpolate the INS and GPS data for the times when laser ranges have been recorded. Interpolation is necessary because the GPS data are recorded at 2 Hz, while laser measurements are recorded every at 500/64 Hz, and INS measurements at 8 Hz.

4. COMPUTATION OF LASER FOOTPRINT

The laser range recorded during the flight is a slant range to the surface. To compute the position of the laser footprint in a global, geographic coordinate system, the laser range, aircraft position, and aircraft attitude are combined according to the scheme described in Lindenberger (1993), Vaughan et al., (1996), and Ridgway et al., (1997). Equation 1 sums up the procedure, which includes a series of coordinate transformations starting at a local reference system centered at the laser firing point (indicated subscript L) and ending in the WGS-84 Cartesian reference frame (indicated subscript W). Rotations are indicated by R (x, y, or z subscripts indicate a rotation about a specific axis).

$$\vec{p}_W^{LPF}(X,Y,Z) = \vec{p}_W^{GPS} + d\vec{p}_W^{GPS} + R_z(-lon^{GPS}) \cdot R_y\left(lat^{GPS} + \frac{\pi}{2}\right) \cdot R(r,p,h) \cdot R(\Delta r, \Delta p, \Delta h)\left(\begin{bmatrix} x_A^{GPS.LFP} \\ y_A^{GPS.LFP} \\ z_A^{GPS.LFP} \end{bmatrix} + R(dp,dr,0) \cdot \begin{bmatrix} 0 \\ 0 \\ r_L^{LFP,S} + \Delta r_{atm} + \Delta r_{bias} \end{bmatrix}\right) \quad \text{(Eqn. 1)}$$

4.1. Range measurement corrections

The laser ranger is mounted inside the aircraft pointing towards nadir. The ranger measures the distance $\left(r_L^{LFP,S}\right)$ between the Laser Firing Point (LFP) and the snow surface (S) from points along the flight trajectory. The measured laser range is corrected for atmospheric delay and a range bias:

- The **atmospheric correction** $\left(\Delta r_{atm}\right)$ accounts for the reduced speed of light and refraction in the atmosphere. It reduces the measured range by approximately 2 cm for every 100 m of altitude. The computation of this correction is taken from Vaughn et al. (1996), Ridgway et al. (1997), and Marini and Murray (1973). Pressure, temperature and water vapor are extrapolated at the aircraft location from data collected by automatic weather stations at Siple Dome and on Ice Stream C. The meteorological data are collected and distributed courtesy of John Stearns of the Automatic Weather Station Project (Stearns, via internet)
- A **range bias** $\left(\Delta r_{bias}\right)$ of 0.35 m is added to each range measurement. This bias is determined by comparing surface elevations derived using laser altimetry to elevations derived using precise surveying methods on the ground (see details in Sect. 5.1). The bias is most likely due to a constant lag in the timing of the laser pulse, although this has yet to be proven and is currently being investigated.

4.2. Transformation from local laser reference system to local Earth tangent reference system

The corrected laser range vector $[0,0,r_L^{LFP,S} + \Delta r_{atm} + \Delta r_{bias}]^{-1}$ is transformed into a local aircraft reference system (indicated subscript A) centered at the GPS antenna. The aircraft reference system is defined using several symmetrical 'hard' points on the aircraft (joists, flap indicators, and seats) whose positions are measured using a theodolite. One axis runs the length of the aircraft between symmetric points. A second axis is perpendicular to the first axis and is aligned with the aircraft wings. The third axis is vertical and perpendicular to the other two. This transformation is carried out by rotating the laser range vector by the laser mounting bias $(dp, dr, 0)$ (see Section 5.2). The offset vector between the laser firing point and the GPS antenna $\left(\left[x_A^{GPS,LFP}, y_A^{GPS,LFP}, z_A^{GPS,LFP}\right]^{-1}\right)$ is then added. The

measured offset of [-1.378, 0.411, 1.566] is found using a theodolite and tape measure.

The next rotation uses the INS mounting biases $(\Delta r, \Delta p, \Delta h)$ to transform the laser vector from the local aircraft reference system into the local INS reference frame with axes defined by the roll, pitch, and heading axes of the INS. The INS mounting biases account for the angular differences between the aircraft body system and the roll, pitch and yaw axes. This step also accounts for the difference between local vertical and the direction perpendicular to the geodetic ellipsoid (WGS-84). SOAR reports a -0.30 degree bias in both pitch and roll. Because these angles are small, the SOAR values are simply added to the attitude angles reported by the INS.

The last rotation of this series transforms the laser vector from the INS reference from to the local-level reference frame using the attitude of the aircraft (r, p, h). The local-level reference frame is an Earth-tangential reference system centered at the GPS antenna. The z-axis is perpendicular to the WGS-84 ellipsoid and points downward. The x-axis lies along the intersection of the local GPS meridian and a plane parallel with the tangent plane to the ellipsoid (i.e., points north). The y-axis completes the right hand system.

4.3. Transformation from local-level reference system to WGS-84 Cartesian system

The laser vector from the GPS antenna to the laser spot on the snow surface is transformed into the WGS-84 global Cartesian system. Rotations for the latitude, $R_y(lat^{GPS} + \frac{\pi}{2})$, and longitude, $R_z(-lon^{GPS})$, of the aircraft are performed to align the local-level reference frame axes with the WGS-84 axes. The final position of the laser footprint is computed by adding the laser vector to the vector recorded by the GPS on board the aircraft. Because the GPS position has uncertainties, some authors (e.g., Lindenberger) use an adjustable parameter ($d\vec{p}_W^{GPS}$) to remove any GPS bias. Lindenberger, (1993), calculated this parameter by surveying a rough but stable surface before and after each flight. Ice sheet surfaces are too flat and not stable enough for this kind of calibration. Other researchers use an adjustment scheme based on the analysis of large set of cross-overs to remove any GPS bias. Our data set does not have enough flights and cross-overs to take advantage of this method either. For these reasons, $d\vec{p}_W^{GPS} = \vec{0}$ is assumed to be zero for this study. After applying simplifications *Equation 1* becomes:

$$\vec{p}_W^{LPF}(X,Y,Z) = \vec{p}_W^{GPS} + R_z(-lon^{GPS}) \cdot R_y\left(lat^{GPS} + \frac{\pi}{2}\right) \cdot R(r+\Delta r, p+\Delta p, h+\Delta h)\left(\begin{bmatrix} x_A^{GPS.LFP} \\ y_A^{GPS.LFP} \\ z_A^{GPS.LFP} \end{bmatrix} + R(dp, dr, 0) \cdot \begin{bmatrix} 0 \\ 0 \\ r_L^{LFP,S} + \Delta r_{atm} + \Delta r_{bias} \end{bmatrix}\right) \quad \text{(Eqn.2)}$$

5. CALIBRATION AND VALIDATION

5.1. Laser range calibration

Two skiways next to the Siple Dome base camp were surveyed using both snowmobile-mounted GPS and laser altimetry in mid-December, 1997 (Figs. 3, 4, and 5).

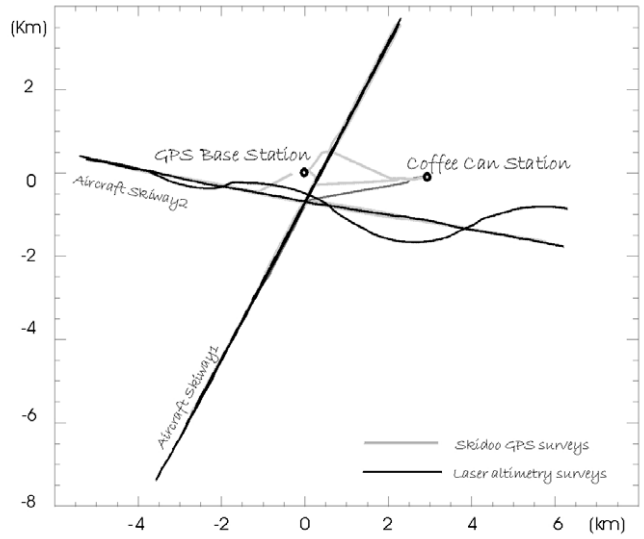

Fig. 3. Laser altimetry calibration surveys at Siple Dome, West Antarctica.

The snowmobile (also referred to as skidoo) surveys are used to produce a reliable surface profile for comparison with laser derived elevations. A +0.35 m bias was found for the laser elevations. This bias is due to a systematic timing error in laser ranging and is added to every laser range during processing. To determine this bias the data are converted into a local, Earth-tangential reference system where the x-axis points to true North, z-axis points toward the center of the Earth, and the y-axis completes a right-hand system. The position of the GPS base station antenna mounted on the SOAR tent was selected as the origin $\left(p_W^{calsite}(X,Y,Z)\right)$. Equation 3 describes the transformation and figures 3, 4 and 5 show how the reference system is used.

$$\vec{p}_{loc}^{LFP}(x_{loc}, y_{loc}, z_{loc}) = R_y(-lat^{calsiteO} - \pi/2) \cdot R_z(lon^{calsiteO}) \cdot (\vec{p}_W^{LFP}(X,Y,Z) - p_W^{calsiteO}(X,Y,Z)) \quad \text{(Eqn.3)}$$

5.2. Laser mounting biases

Due to mounting errors, the laser is not perfectly aligned with the aircraft's roll and pitch axes, as defined by the INS. The laser mounting bias is defined as the angular difference between the aircraft body and the laser axes. The estimated laser mounting bias is -1.2 degrees in pitch and -0.3 degrees in roll during the 1997/98 field season (SOAR field notes). Pitch and roll maneuvers over a relatively flat test field are used to check these values. The deformed surface shown in Figure 5 is the result of a laser survey where no mounting bias corrections were used. By changing *dr* and *dp* to minimize the surface

deformation the mounting bias can be estimated. In this case the initial estimate of -1.2 degree in pitch and - 0.3 degree in roll was confirmed by using a simple grid search.

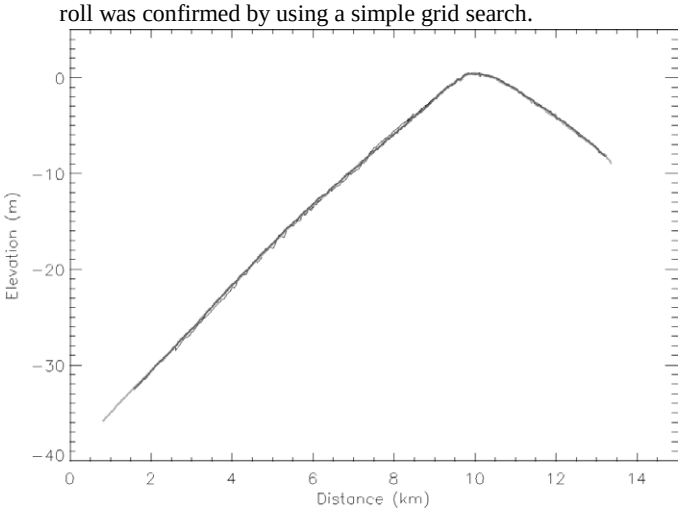

Fig. 4. Surface derived from repeat laser altimetry (grey lines) and snowmobile-mounted GPS (thin black lines) along Skiway1.

5.3. System Accuracy

After correction of range and angular biases the SOAR system performed well over short distances. Repeat flights over Skiway1 show a 2.8 cm bias with an overall RMS of 10.3 cm. The bias is attributed to surface slope, because the repeat flight lines were approximately 25 m apart. The RMS difference is measurement of surface roughness caused by sastrugi. Sub-decimeter accuracy was also found when laser derived elevations were compared to elevations measured with the snowmobile surveys.

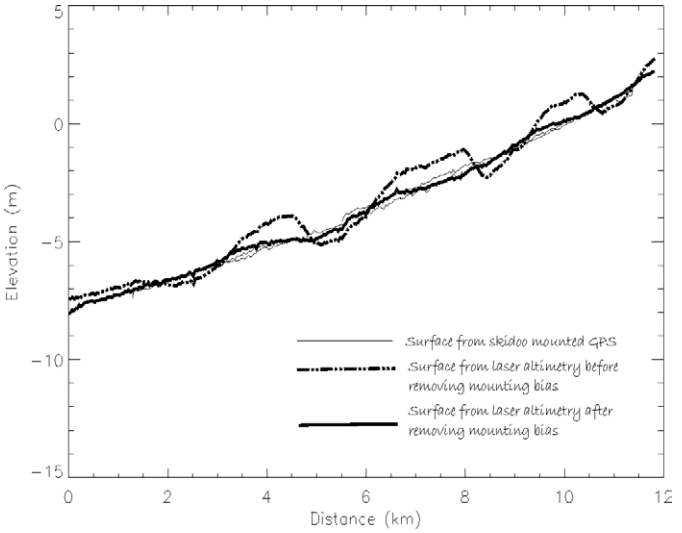

Fig. 5. Comparison of measured elevations along Skiway 2 surveyed with snowmobile-mounted GPS and laser altimetry. The two laser profiles are derived from the same survey before and after the removal of the laser mounting bias. The magnitude of the pitch maneuvers are about 8 degrees off nadir.

6. REPEATABILITY AND ACCURACY

6.1. Crossing flight lines

Laser surveys that cross nearly perpendicular to one another are evaluated to determine the repeatability of the procedure over long baselines. Crosses are evaluated by finding laser measurements within a 10 m radius of the cross-over point. The average elevation difference of crosses on Ice Stream C are shown in Table 1. Table 1 also shows how crosses compare if both laser surveys were conducted during the same or independent GPS surveys. The agreement is better for crosses measured during the same flight.

Elevations produced from Ice Stream C survey flight number *26* were found to have large biases of up to 84 cm. This large bias is 8 times greater than the reported GPS RMS for that flight, which suggests that the phase ambiguities were not resolved throughout the entire flight. Poor GPS initialization practices (i.e. the aircraft started and ended at different base camps over 280 km apart) are the most likely source of the problem. The end result is that the flight is of limited use for change detection on a two year time-scale, and topographic maps made with this flight could have an error of nearly a meter. Average elevation differences are given for Ice Stream C with and without this flight (Table 1).

Surveys Considered	*Number of Crosses*	*Number of Laser Measurements*	*Mean Elevation Difference Between Surveys*
All surveys	8	34	0.36 m
w/o *26*:	4	16	0.25 m*
Same GPS Survey	2	8	0.18 m*
Independent GPS survey	2	8	0.32 m*

** Values do not include measurements from survey flight 26.*

Table 1. Cross-over comparisons for Ice Stream C

6.2. Coffee-can comparisons

Laser surveys go near distant coffee can stations providing a means for evaluating accuracy over long baselines (Fig. 6). The coffee-can markers are surveyed using precision GPS methods and are used to study ice sheet mass balance (Hamilton et al., 1998). GIPSY is used to determine marker positions with a vertical error of less than 0.01 m. The laser flights missed the coffee can site on Ice Stream C by 840 m,

therefore linear interpolation is used to estimate laser elevations at the coffee can site. Results showed that laser elevations agreed to within 0.10 m of the coffee can elevation.

7. TOPOGRAPHIC MAPS

Large portions of ice streams B1, B2, C, and E have been surveyed. Topographic maps have been made for all four ice streams with varying uncertainties. An example is shown in Figure 6 for Ice Stream C. Ice surface contours compare very well with an earlier radar study (Retzlaff et al., 1993), although the older maps have uncertainties that are too large to be useful for detection of changes in surface elevation. The laser derived surface map is superimposed over bed elevations taken from radar measurements (Fig. 6) to show how bed features affect the ice in terms of velocity vectors, surface elevations, and slope.

8. GLACIOLOGIC INTERPRETATION

Ice Stream C was chosen as a likely location for rapid ice thickness change because the downstream portion is nearly stagnant while the upstream portion is still active (Fig. 6). Within the laser grid, the ice velocities go from 25 m/a to 3 m/a (Whillans and Van der Veen, 1993 and Joughin et al., 1999). As more ice moves into the region, ice thicknesses are expected to increase by 0.50-1.0 m/a (Whillans and Van der Veen, 1993 and Joughin et al., 1999). Figure 6 also shows that surface slopes are greater in the zone where velocity decreases the quickest. This is an impossible scenario for steady-state conditions and could be evidence that Ice Stream C is being reactivated. It seems sensible that a build-up of ice will cause the ice to begin streaming again.

The pattern of ice thickness, ice velocity, and surface slope observed on Ice Stream C are unlike what is normally expected. Ice thickness decreases by a factor of two from the upstream portion of the grid to the downstream portion mostly as a result of increased bed elevations. The velocity decreases by a factor of four for the same region and the surface slope increases by a factor of 2. In an ordinary glacial setting, the velocity would increase with increased surface slope and decreased thickness. The ice seems to be piling up as it reaches the bedrock ridges. This could be due to a lack of subglacial water at the downstream end. If the upstream portion of the ice stream is sliding over clay-rich sedimentary rocks, basal friction would be very small for two reasons. First, ice thicknesses are great enough in this region to induce pressure melting despite cold temperatures. Second, clay rich materials have very low permeabilities so water is not able to escape. This scenario has been shown to exist beneath other fast flowing ice streams (Anandakrishnan and Bentley, 1993; Engelhardt et al. 1990). As for the downstream portion of Ice Stream C, Anandakrishnan and Bentley (1993) found basal seismic noises that were not sensed beneath fast flowing ice streams. The interpretation was that Ice Stream C must have experienced a dewatering and loss of dilatency in the lubricating till layer. Without well-distributed water the ice can become frozen to the bed, forming 'sticky' spots, or in this case an entire 'sticky' region. The future course of the growing bulge will determine the behavior of ice stream C and will illustrate the effect of glaciologic processes, presumably the advancement of a lubricated bed. One can expect a major change of the studied region as this thickening continues.

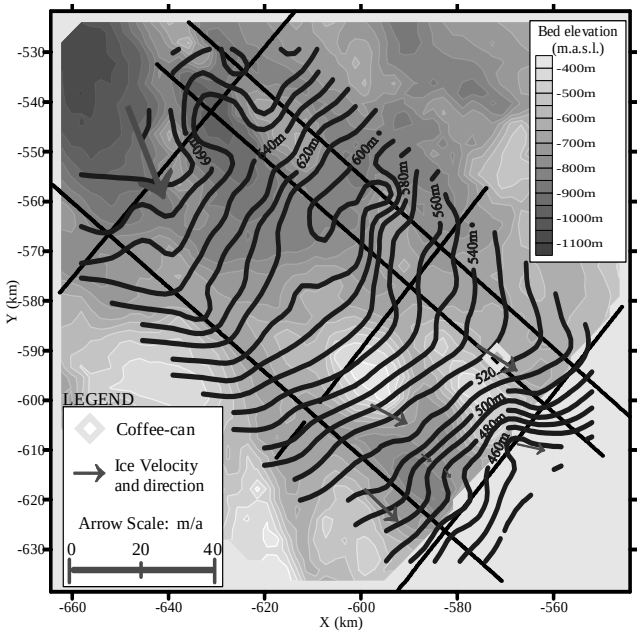

Fig. 6. Laser derived elevation contours (blue) of the surface of Ice Stream C superimposed over bed elevations from airborne radar surveys (Taken from Retzlaff et al., 1993). Red arrows show ice flow direction and magnitude (Taken from Whillans and Van der Veen, 1993, and Hamilton, pers. comm.). The yellow diamond is a coffee-can site whose known elevation is used to validate laser derived elevations (Hamilton, pers. comm.). Dashed black line shows the track of the laser surveys.

9. CONCLUSIONS

At the onset of this project it was expected that uncertainties would be at least 1-meter. The large uncertainties were expected to come from the GPS solutions because the GPS satellites that cover Antarctica are at low angles making it difficult to resolve errors in the vertical. Uncertainties in the 10 to 30 centimeter range were found instead. Most elevations from crossing flight lines compare within 20 cm during the same GPS survey and within 30 cm for crosses involving two separate GPS surveys. This level of precision is acceptable, but could probably be improved with better GPS surveying techniques. These would include static initialization at the beginning and end of each survey, beginning and ending flights at the same base camp, and more surveys conducted on the snow surface for bias determination. Nevertheless, this level of precision will allow changes in ice sheet elevations to be detected in the 2 year time interval for most of the study region. Laser altimetry is shown here to be a valuable tool for mass balance measurement for all of Antarctica. It is also shown to be a useful tool in locating unusual topographic features that can lead to a greater understanding of glacier mechanics.

ACKNOWLEDGEMENTS

We would like to thank John Sonntag for helping validate our GPS surveys, Dorota Grejner-Brzezinska for helping in processing the GPS data, and SOAR for acquiring the laser data and helping with processing concerns. Funding for this project is provided by National Science Foundation grant OPP-9615114.

REFERENCES

[Adalgeirsdóttir et al., 1998] Adalgeirsdóttir, G., Echelmeyer, K. Harrison, W., 1998. Elevation and volume changes of Harding Icefield, Alaska. J. Glaciology, 44 (148), pp. 570-581.

[Anandakrishnan and Bentley, 1993] Anandakrishnan, S., and Bentley, C., 1993. Micro-earthquakes beneath Ice Streams B and C, West Antarctica: observations and implications. Journal of Glaciology, 39 (133), pp. 455-462.

[Bindschadler and Vornberger, 1998] Bindschadler, R., and Vornberger, P., 1998. Changes in the West Antarctic Ice Sheet since 1963 from declassified satellite photography. Science, 279, p. 689-692.

[Csatho et al., 1996] Csatho, B., Schenk, T., Thomas, R., and Krabill, W., 1996. Remote sensing of polar regions using laser altimetry. International Archives of Photogrammetry and Remote Sensing. XXXI (B1), pp. 42-47.

[Echelmeyer et al., 1996] Echelmeyer, K., Harrison, W., Larsen, C., Sapiano, J., Mitchell, J., DeMallie, J., Rabus, B., Adalgeirsdottir, G., Sombardier, L., 1996. Airborne surface profiling of glaciers: A case study in Alaska. J. Glaciology, 42 (142), pp. 538-547.

[Engelhardt, 1990] Engelhardt, H., Humphrey, N., Kamb, B., Fahnestock, M., 1990. Physical conditions at the base of a fast moving Antarctic ice stream. Science, 248 (4951), pp. 57-59.

[Garvin and Williams, 1993] Garvin, J. and Williams, R., 1993. Geodetic airborne laser altimetry of Bredamerkurjökull and Skeidarárjökull, Iceland, and Jakobshavns Isbrae, West Greenland. Annals of Glaciology, 17, pp. 379-385.

[Hamilton et al., 1998] Hamilton, G., Whillans, I., Morgan, P.J., 1998. First point measurements of ice sheet thickness change in Antarctica. Annals of Glaciology, 27, pp. 125-129.

[Joughin et al., 1999] Joughin, I., Gray, L., Bindschadler, R., Price, S., Morse, D., Hulbe, C., Karim, M., and Werner, C., 1999. Tributaries of West Antarctic ice streams by RADARSAT interferometry. Science, 286, pp. 283-286.

[Krabill et al., 1995] Krabill, W., Thomas R., Martin, C., Swift, R., and Frederick, E., 1995. Accuracy of airborne laser altimetry over the Greenland ice sheet. Int. J. Remote Sensing, 16 (7), pp. 1211-1222.

[Krabill et al., 1999] Krabill, W., Frederick, E., Manizade, S., Martin, C., Sonntag, J., Swift, R., Thomas, R., Wright, W. and Yungel, J, 1999. Rapid thinning of parts of the southern Greenland ice sheet. Science, 283, pp. 1522-1524.

[Lindenberger, 1993] Lindenberger, 1993. Laser-Profilmessungen zur topographischen Geländeaufnahme. Ph. D. Dissertation, Universität Stuttgart, Verlag der Bayerischen Akademie der Wissenschaften, 131 pages

[Marini and Murray, 1973] Marini, J., and Murray, C., 1973. Correction of laser range tracking data for atmospheric refraction at elevation angles above 10^{o}. NASA Technical Report, X-591-73-351, NASA/Goddard Space Flight Center.

[Mullins, 1999] Mullins, J. L., 1999. The geodesy and mapping program of the United States Geological Survey in Antarctica. PERS, 65(12), pp. 1340-1341.

[Retzlaff et al., 1993] Retzlaff, R., Lord, N., and Bentley, C., 1993. Airborne-radar studies: Ice Streams A, B and C, West Antarctica. J. Glaciology, 39(133), p. 495.

[Ridgway et al., 1997] Ridgway, J., Minster, J., Williams, N., Bufton, J., and Krabill, W., 1997. Airborne laser altimetry survey of Long Valley, California. Geophys. J. Int., 131, pp. 267-280.

[Shi and Cannon, 1995] Shi, J., and Cannon, M.E., 1995. Critical error effects and analysis in airborne DGPS positioning over large areas. Manuscripta Geodaetica, 69, pp. 261-273.

[Stearns, via internet] Charles Stearns, P.I., Automatic Weather Station Project, University of Wisconsin-Madison, http://uwamrc.ssec.wisc.edu/aws.

[Vaughn et al., 1996] Vaughn, C., Bufton, J., Krabill, W., and Rabine, D., 1996. Georeferencing of airborne laser altimetry measurements. Int. J. Remote Sensing, 17(11), pp. 2185-2200.

[Whillans and Van der Veen, 1993] Whillans, I. and Van der Veen, C., 1993. New and improved determinations of velocity of Ice Streams B and C, West Antarctica. 39(133), pp.483-490.